

# We are IntechOpen, the world's leading publisher of Open Access books Built by scientists, for scientists

6,900

Open access books available

186,000

International authors and editors

200M

Downloads

Our authors are among the

154

Countries delivered to

TOP 1%

most cited scientists

12.2%

Contributors from top 500 universities



WEB OF SCIENCE™

Selection of our books indexed in the Book Citation Index  
in Web of Science™ Core Collection (BKCI)

Interested in publishing with us?  
Contact [book.department@intechopen.com](mailto:book.department@intechopen.com)

Numbers displayed above are based on latest data collected.  
For more information visit [www.intechopen.com](http://www.intechopen.com)



# Synthesis of Pt – Containing Metals Alloy and Hybrid Nanowires and Investigation of Electronic Structure Using Synchrotron-Based X-Ray Absorption Techniques

Xiaowei Teng<sup>1</sup>, Wenxin Du<sup>1</sup> and Qi Wang<sup>2</sup>

<sup>1</sup>University of New Hampshire,

<sup>2</sup>University of Delaware

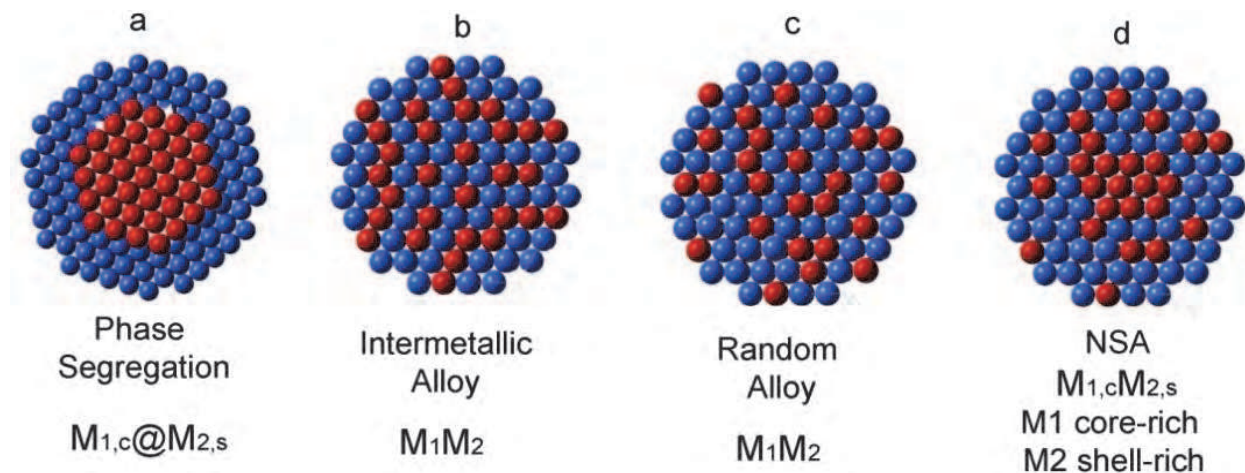
USA

## 1. Introduction

Platinum-containing bimetallic nanomaterials have shown different electronic structures from their monometallic counterparts, bringing exotic properties to various catalytic and magnetic applications. The synthesis and shape-dependent properties of bimetallic cubes, truncated cubes, dendrites, and hollow structures, have been intensively studied. One dimensional (1D) Pt-containing nanostructure has attracted special interest, although synthetic challenges in the fine control over morphology arising from unfavorable anisotropic growth of symmetric cubic lattice structures from Pt metal and alloys (Ahmadi et al., 1996; Cozzoli & Manna, 2005; Xia et al., 2003).

The electronic structure of bimetallic nanowires is associated with their heterogeneous structural diversity strongly, such as phase segregation (Zhong & Maye, 2001), intermetallic alloy (Casado-Rivera et al., 2004), random alloy (Shibata, et al., 2002) and near surface alloy (NSA) (Greeley & Mavrikakis, 2006; Knudsen, et al., 2007) (See Scheme). Therefore, detailed studies of bimetallic heterogeneous structures are essential for their applications. The structural characterization of bimetallic nanomaterials is not trivial, partly due to the complexity of heterogeneous nature imposed by nanoscale system. X-ray absorption fine spectroscopy (XAS) is a well established tool for investigating the element-resolved structure of bimetallic nanomaterials, since the local environment and electronic properties of atoms of each resonant element can be studied separately by tuning the X-ray energy to the absorbing edge of each metal. XAS has been successfully used to study bonding habit, geometry, electronic and surface structure of many bimetallic nanoparticles (e.g., Pt/Ru, Pt/Au, Pd/Au and Pt/Ir) (Nashner et al., 1997). When the short range order information extracted from XAS analysis is combined with the knowledge of the long range order and average compositional distribution obtained by complementary techniques, actual heterogeneous structure and electronic state of nanomaterials can be quantitatively analyzed.

In this chapter, we intend to focus on our recent results on the synthesis and electronic structures of ultrathin PtAu alloy nanowires, Pt/Au phase-segregated hybrid nanowires.



**Scheme** Four heterogeneous nanostructures: (a) Phase segregation (surface of metal  $M_1$  is modified by irreversibly adsorbed  $M_2$ ); (b) Intermetallic alloy (atoms  $M_1$  and  $M_2$  are mixed with definite lattice proportions); (3) Random alloy (homogeneous alloy, atoms  $M_1$  and  $M_2$  are mixed statistically in accordance with the overall concentration). (4) NSA alloy (atoms  $M_1$  are core-rich and  $M_2$  are shell-rich)

The PtAu alloy and Pt/Au hybrid nanowires with average width less than 3 nm and length over 50 nm were made from phase transfer method, in which inorganic gold and platinum precursors were transferred into an organic mixture via phase transfer agent. Subsequent injection of the reducing agent resulted in the formation of nanowires. Generally, the anisotropy of crystal structure is believed to be the main driving force for the anisotropic growth of nanostructures. However, this would not be the case accounting for formation of PtAu nanowires or Pt nanowires upon which Au particles grow to create Pt/Au hybrids, as both Pt and Au are isotropic in crystal lattice structure. Unlike the cases in quantum dots where the dipole moment was the driving force, the anisotropic growth of these Pt and PtAu nanowires is most likely due to the kinetics control of the growth rates of various facets of seeds driven by specific binding of capping agent on specific crystal surfaces. The tentative growth mechanisms to each subcategory PtAu nanowires or hybrid nanowires will be presented.

In addition to the synthesis, crystalline and electronic structure of those nanowires will be determined by various techniques, including transmission electron microscopy (TEM) and energy dispersive spectrometry (EDS), etc. The disclosure of morphology and crystalline details of those homogenous/heterogeneous bimetallic nanowires will be mainly relied on TEM and HRTEM equipped with EDS as well as EXAFS analysis. UV-vis spectroscopy is specifically used to find out the existence of Au in PtAu nanowires and possible size effect. The electronic structure, the charge transfer between the each component throughout the bimetallic nanowires in particular, will be determined by synchrotron-based X-ray absorption spectroscopy (XAS). The relationship between the heterogeneous structure and the electronic properties of the bimetallic nanowires will be studied. Our studies on the synthesis and electronic structure of Pt-containing nanowires will be highly encouraging new families of bimetallic nanowires systems. Such research may be developed to sustain the needs of emerging technologies such as renewable energy and spintronics, where there is a continuous drive to find nanomaterials with ever more exotic

electronic and catalytic properties, and where the assembly of these fundamental building blocks can lead to new types of functionality. The new electronic structure driven by enhanced charge transfer between heterogeneous atoms will continue to be our focus in the future.

## 2. Synthetic strategy of Pt-containing nanowires

There are a variety of chemical methods to be able to generate 1D nanostructures including nanowires. Although the general methods for growing 1D nanostructures still yet available, a number of strategies are readily for employ, including utilization of anisotropic crystalline structure of a material to facilitate 1D growth, introduction of a liquid-solid interface to reduce the symmetry of a seed, template-directed 1D nanostructure formation, modification of growth habit of seeds by supersaturation control, kinetic control over various facets of seeds by adding suitable capping agents, self-assembly of 0D nanostructures and size reduction of 1D microstructures. The anisotropy of crystal structure is believed to be the main driving force for the anisotropic growth of nanostructures in liquid phase synthesis. However, since both Pt and Au have symmetric cubic lattice, it is intrinsically difficult to make nanowires from these materials. In the following sections, we will show the readers our strategy to synthesize a variety of Pt and Pt/Au nanowires structures by careful selection of synthetic methods as well as manipulations of experimental conditions.

### 2.1 Synthesis of Pt nanowires

The liquid phase synthesis is commonly used for metal salt reduction, either in homogenous system or two phase systems. Here, we chose phase transfer method (Brust et al., 1994), i.e. two phase synthesis to make Pt-containing nanowires with different morphologies and electronic structures. One of the big advantages of this method is that by using relatively simple and inexpensive inorganic metal precursors, we are able to harvest nanomaterials with controllable size and shape as well as hydrophobic properties at room temperature. Typically, the metal ions are first extracted from an aqueous solution to a hydrocarbon (toluene) phase with the help of a phase-transfer agent such as tetraoctylammonium bromide (DTAB). Then further reduction occurs upon adding aqueous sodium tetrahydroborate ( $\text{NaBH}_4$ ) in the presence of an alkanethiol or alkylamine as surfactant. The nucleation and growth of these metal particles and the attachment of the thiol or amine molecules to the nanoparticles would occur simultaneously in a single step. In the synthesis of Pt nanowires, inorganic platinum chloride ( $\text{PtCl}_2$ ) or sodium hexachloroplatinate ( $\text{Na}_2\text{PtCl}_6$ ) was transferred to a mixture of surfactant octadecylamine (ODA) and toluene using phase transfer agent DTAB. Now the surfaces of metal ions were capped with ODA and DTAB as shown in Step One in Figure 1. After injection of overdosed  $\text{NaBH}_4$  in aqueous solution, platinum ions were reduced rapidly under such a highly reductive environment to form thermodynamically unstable elongated primary nanostructures (PN), which is depicted in Step Two (Figure 1). At the same time, the secondary growth of PN apparently took preferred equivalent directions also along  $\langle 111 \rangle$ , leading to the attachment growth of thread-like quasi-nanowires (Step Three, Figure 1). Considering the obvious absence of crystal structure anisotropy of Pt, the oriented attachment in these Pt nanostructures was most likely due to the selective growth driven by specific binding of capping agent on specific crystal surfaces. In general, the shape of nanomaterials is highly dependent on the

competitive growth rate along the low index crystal planes in the presence of surfactants. Alkaline seemed to preferentially adsorb on the surfaces of Pd and Pt, and facilitate the growth of PNs along  $\langle 111 \rangle$  directions.

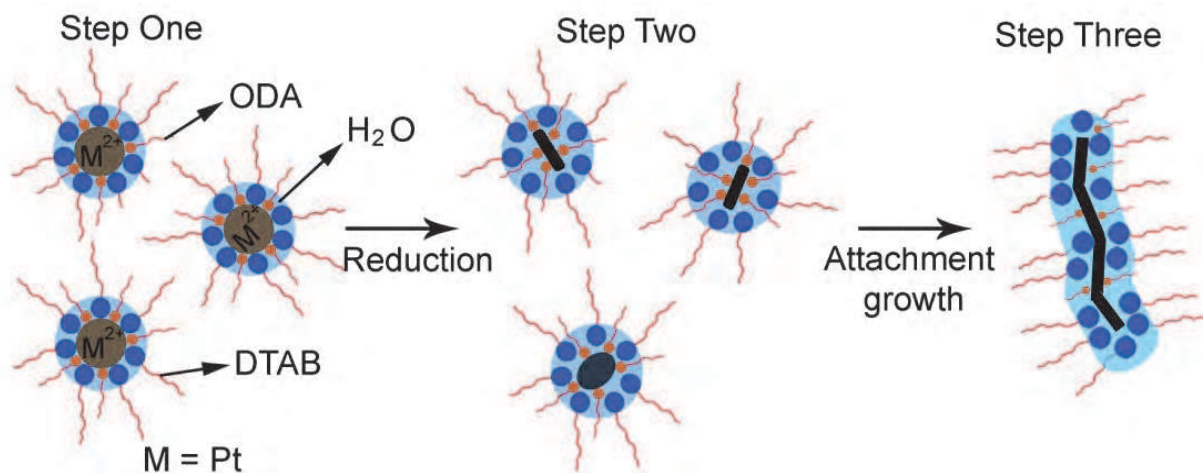


Fig. 1. Schematic diagram of the formation of Pt nanowires.

## 2.2 Synthesis of Pt/Au alloy nanowires

Similar as in the synthesis of Pt nanowire, making Pt/Au alloy nanowires also faces the same challenge to direct the unfavorable anisotropic growth due to the isotropic crystal lattice of Pt and Au. Although the reduction potential of Au<sup>3+</sup> to Au is higher than that of Pt<sup>2+</sup> to Pt in general, it is still possible to get Pt/Au alloy formation under highly reducing environment. Based on the successful experience of synthesis of Pt nanowires, we obtained Pt/Au nanowires via the same phase transfer method. In contrast to the synthesis of Pt nanowires, the Pt/Au alloy nanowires were made by co-reduction of two inorganic precursors, in which AuCl<sub>3</sub> and sodium tetrachloroplatinate (Na<sub>2</sub>PtCl<sub>4</sub>) were transferred into an organic mixture of octadecylamine and toluene via a phase transfer agent DTAB. Subsequent injection of the reducing agent NaBH<sub>4</sub> aqueous solution resulted in the formation of ultrathin Pt/Au nanowires. Eventually, two alloyed ultrathin nanowires, Pt<sub>75</sub>Au<sub>25</sub> and Pt<sub>52</sub>Au<sub>48</sub>, were identified and analyzed later on.

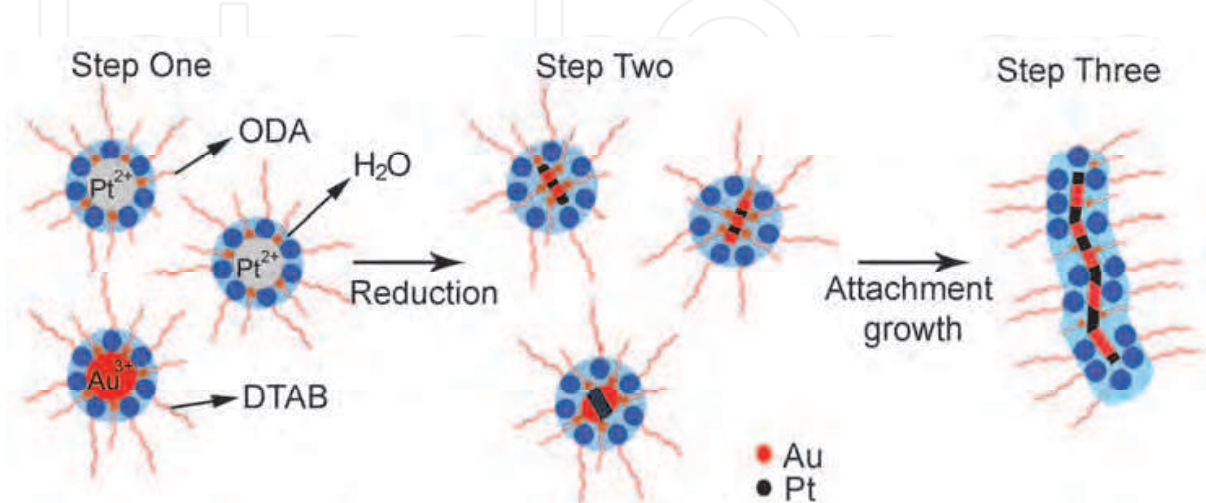


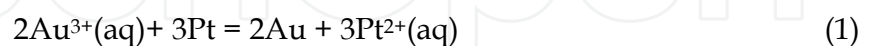
Fig. 2. Schematic diagram of the formation of Pt/Au alloy nanowires.

Compared to Pt nanowires formation, the growth mechanism of Pt/Au alloy nanowires would be similar without considering the distributions of Pt and Au atoms within the Pt/Au nanowires. Figure 2 sketches out the simplified formation process of Pt/Au alloy nanowires. In fact, the detailed Pt/Au nanowires structures exhibit stoichiometry-dependency. It is demonstrated later that Pt<sub>75</sub>Au<sub>25</sub> and Pt<sub>52</sub>Au<sub>48</sub> nanowires are alloyed structures, with the latter having homogeneous placement of Au and Pt atoms and the former a more highly ordered arrangement, with a Pt-rich shell and an Au-rich core. It is interesting to consider how the heterogeneous Pt<sub>75</sub>Au<sub>25</sub> alloy nanowires initially formed and how they subsequently evolved into homogeneous Pt<sub>52</sub>Au<sub>48</sub>. Here, we propose a growth mechanism which explains the formation of Pt/Au nanostructures with such a strong sensitivity to Pt/Au stoichiometry. In the synthesis of Pt/Au alloy nanomaterials, we believe that the standard reduction potential and surface free energy are the most important intrinsic parameters for determining the final heterogeneous nanostructures, and lead to two competing mechanisms for the distribution of Au and Pt within the growing nanowire. On the one hand, the high values of standard reduction potential of Au and Pt in solution at room temperature ( $E^\Phi(\text{Pt}^{2+}/\text{Pt}) = 1.20 \text{ V}$ ,  $E^\Phi(\text{Au}^{3+}/\text{Au}) = 1.52 \text{ V}$ ) suggest that the Au<sup>3+</sup> and Pt<sup>2+</sup> ions are reduced quickly by the addition of excess amounts of NaBH<sub>4</sub> during the synthesis. However, since the reduction potential of Au is slightly higher than that of Pt, it is plausible that Au<sup>3+</sup> would be reduced more easily during the nucleation and consequent growth stages, and would consequently be found in the core, which forms first. On the other hand, surface free energy, in fact defined by the change of the free enthalpy of the surface-creating process under an isothermal-isobaric condition, gives rise to an opposite trend for the Pt/Au atomic distribution compared to the reduction potential. The surface free energy of Au at room temperature (1.63 J/m<sup>2</sup>) is much lower than that of Pt (2.69 J/m<sup>2</sup>). This argument would then conclude that Au atoms would cluster near the surface of the product, while the Pt atoms are relegated to the sublayer or core region.

These competing growth mechanisms based on the standard reduction potential and surface free energy, are further complicated by the interaction between metal surface and capping agent. It is well known that the capping agent (surfactant) is very important in the formation of nanomaterials during solution phase synthesis. For instance, alkaline carboxylic acids, alkylamines, alkylthiols and alkylphosphines have all been used for the synthesis of transition metal/alloy and semiconductor nanomaterials with fine control over size, shape and composition. The interaction between the surfactant and the metal surface is largely dependent on the electronegativity of the metal. Electronegativity describes the power of an atom to attract electrons to it. Fluorine (the most electronegative element) is assigned a value of 4.0, while cesium and francium which are the least electronegative, have electronegativities of only 0.7. Since electronegativities of various atoms differ as following: O > N > S > Au > Pd > Pt, Pt atoms are then expected to show a relatively stronger interaction with octadecylamine (C<sub>18</sub>H<sub>36</sub>NH<sub>2</sub>) than Au atoms, following from the increased probabilities of charge transfer from Pt and Au atoms to N atoms. As a consequence of preferential binding between octadecylamine and Pt metals surfaces, we suggest that the Pt atoms will be stabilized toward the surface and Au atoms diffuse into core region, accounting for the formation of an Au<sub>C</sub>Pt<sub>S</sub> (Au-core-rich and Pt-shell-rich) heterogeneous alloy. In fact, preferential binding between alkylamine or alkylthiol with Pd atoms have previously been reported to account for the formation of Au<sub>C</sub>Pt<sub>S</sub> non-random alloy.

### 2.3 Synthesis of Pt/Au hybrids based on Pt nanowires

Considering that the standard reduction potential of Au is higher than Pt in solution at room temperature ( $E^\Phi(\text{Pt}^{2+}/\text{Pt}) = 1.20 \text{ V}$ ,  $E^\Phi(\text{Au}^{3+}/\text{Au}) = 1.52 \text{ V}$ ), it is plausible to utilize galvanic replacement reaction between  $\text{Au}^{3+}$  and Pt nanowire to obtain hybrid structures. When two metals satisfy such condition, i.e. the one with lower reduction potential exists in metallic state and the other with higher reduction potential stays as ion, the latter tends to seize electrons from the former, making itself being reduced and leaving the former metal being oxidized and thus dissolved in solution. Indeed, the Pt/Au hybrid nanowires were successfully acquired upon the galvanic replacement reaction between  $\text{AuCl}_3$  and as-made Pt nanowires as indicated by following reaction:



After fresh Pt nanowires were made,  $\text{AuCl}_3$  solution was prepared by dissolving in toluene in the presence of relatively small amount of DTAB. The different volumes (0.4, 1.0, 2.0 ml) of  $\text{AuCl}_3$  solution (40 mM) was then injected into fresh made Pt nanowire solution ( $\sim 0.06 \text{ mmol}$ ) to form 3 types of nanostructures. The galvanic replacement reaction proceeded for one hour under argon protection at room temperature.

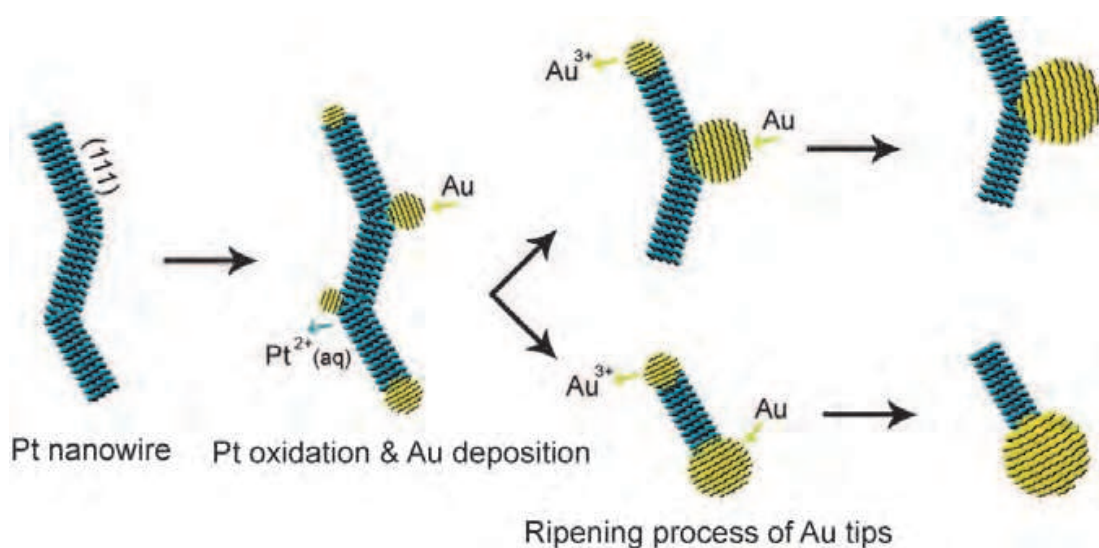


Fig. 3. Schematic drawing of the galvanic replacement reaction between Pt nanowires and  $\text{Au}^{3+}$ .

The proposed growth mechanism of Pt/Au hybrid nanowires formation is presented in Figure 3. When  $\text{AuCl}_3$  was added to the solution containing ultrathin Pt nanowires,  $\text{Au}^{3+}$  ions might preferentially attach to the certain sites along the Pt nanowires such as tips, stacking faults, and twinning boundaries, since those sites possess higher surface energy and/or relatively less passivation by surfactants due to rather sharp radius of curvature. Since the reduction potential of  $\text{Au}^{3+}$  to Au ( $E^\Phi = 1.5 \text{ V}$ ) is higher than that of  $\text{Pt}^{2+}$  to Pt ( $E^\Phi = 1.2 \text{ V}$ ), Pt nanowires were oxidized and  $\text{Au}^{3+}$  ions were then reduced by the electrons generated from the replacement reaction. As the reaction continued, the Au nanoparticles grew larger, along with the consumption and breakdown of Pt nanowires. The Ostwald ripening process may also occur during the galvanic replacement reaction, accounting for the disappearance of smaller Au components to facilitate the growth of larger Au components. The ripening of Pt nanowires, however, was not preferred as evidenced by the fact that the width of Pt nanowires did not change.

### 3. Morphology and crystalline structures of Pt-containing nanowires

To decipher the morphology and crystalline structures of Pt/Au nanowires, and electronic structures of those Pt-based nanowires, advanced characterization techniques, including transmission electron microscopy (TEM), scanning transmission electron microscopy (STEM) equipped with X-ray energy dispersive spectroscopy (EDS) or ultraviolet-visible (UV-vis) spectroscopy, and extended X-ray absorption fine structure (EXAFS) spectroscopy, were combined selectively to study these nanomaterials. In particular, the EXAFS appears as a powerful tool to provide precise crystalline details in average within the nanowires. These detailed structure information will help us obtain an insight on the exotic electronic structures in these Pt/Au nanowires.

#### 3.1 TEM and STEM-EDS analysis

The morphologies and crystalline structure of Pt nanowires can be clearly seen in Figure 4.

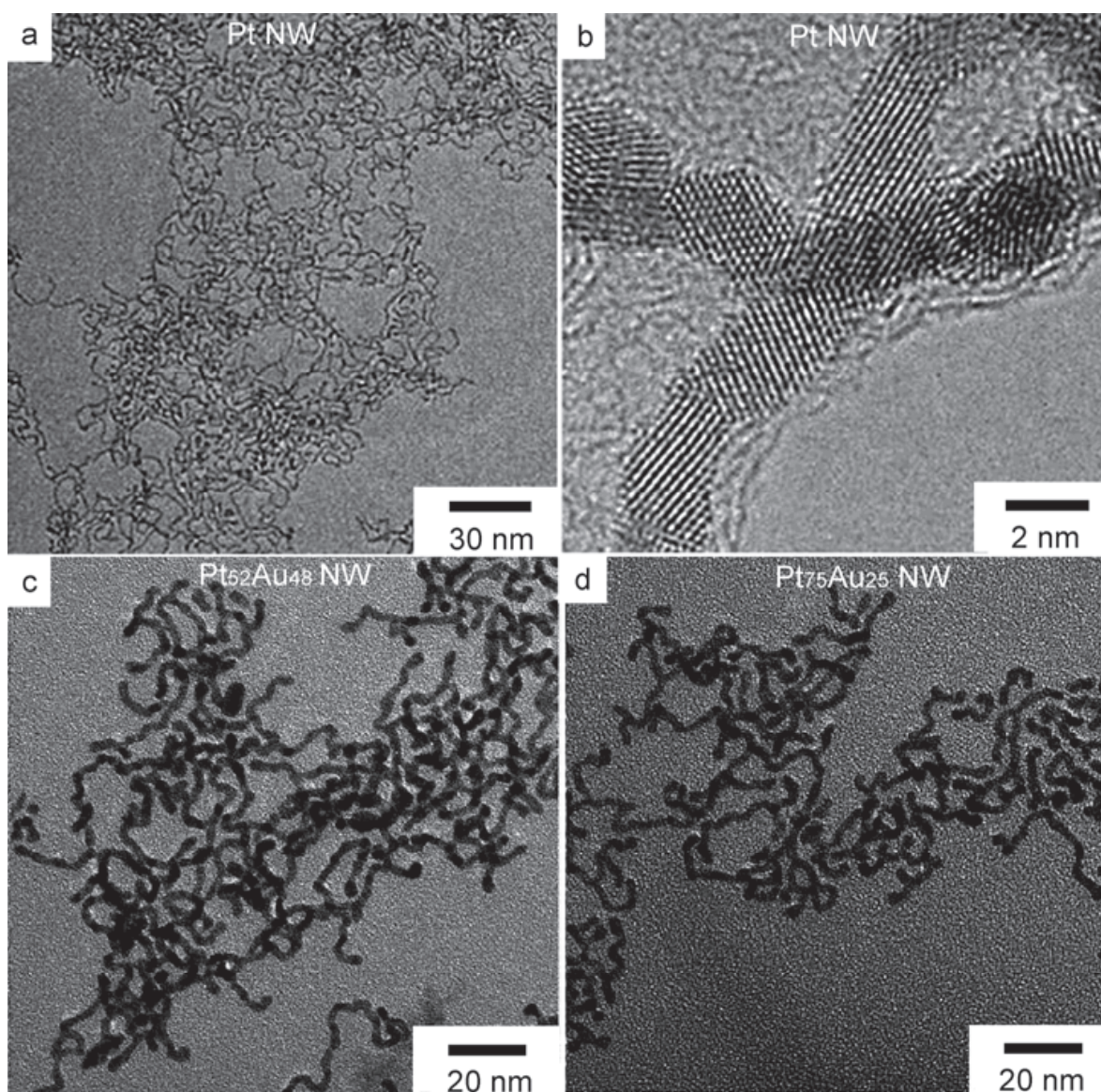


Fig. 4. TEM images of (a, b) Pt nanowires, (c) Pt<sub>52</sub>Au<sub>48</sub>, and (d) Pt<sub>75</sub>Au<sub>25</sub> nanowires.

Figure 4a shows the as-made Pt nanowires with dimension of  $2.3 \pm 0.2$  nm in width and over 30 nm in length. High-resolution TEM (HRTEM) shows Pt nanowires are polycrystalline with well-defined lattice planes, both twinning boundaries and stacking faults are observed (Figure 4b). HRTEM reveals that each nanowire is composed of several single-crystalline, elongated primary nanostructures (PNs) and the secondary growth of PNs apparently took preferred equivalent directions also along  $\langle 111 \rangle$ .

The Pt<sub>52</sub>Au<sub>48</sub> and Pt<sub>75</sub>Au<sub>25</sub> alloy nanowires which were synthesized via co-reduction of Pt and Au metal precursors, exhibited a uniform 1D morphology, with average lengths as large as 100 nm, average widths of  $2.6 \pm 0.4$  nm and  $2.5 \pm 0.3$  nm, respectively (Figure 4c, 4d). These Pt/Au nanowires appeared to be entirely crystalline, evidenced by the lattice fringes which extend across the full extent of the TEM image. Dominant lattice spacing of 2.3 Å were obtained, which corresponds to the interplanar distances of the  $\{111\}$  Pt/Au surfaces (data are not shown). In general, the shape of materials is highly dependent on competitive growth along the low index crystal planes in the present of surfactant, including (111), (110) and (100) planes. Anisotropic growth of Pt/Au nanowires is rather unexpected due to the symmetric cubic lattices of both Pt and Au metals. However, our TEM data indicate that octadecylamine might preferentially adsorb on the surfaces of Au and Pt, facilitating the growth of Pt/Au nanowires along the  $\langle 111 \rangle$  directions.

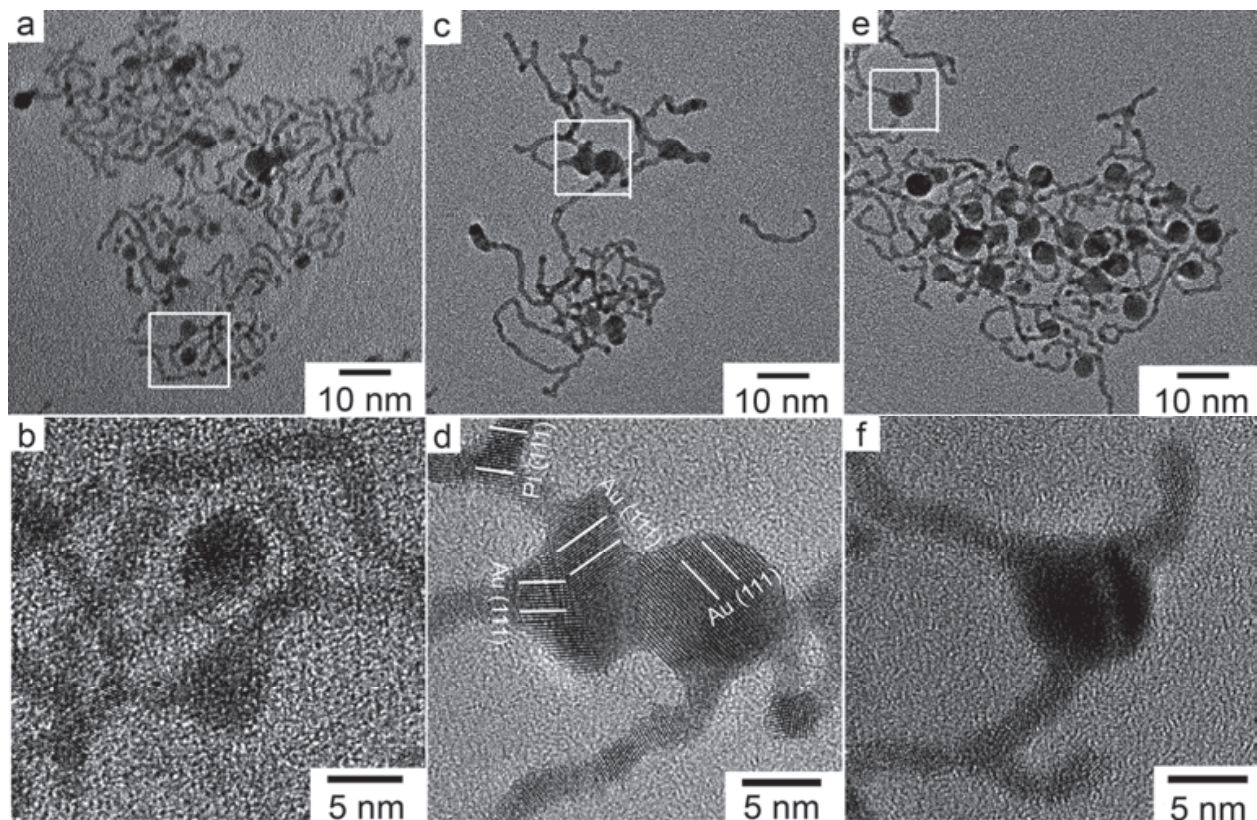


Fig. 5. TEM images of Pt/Au hybrid nanowires obtained by titrating the Pt nanowires with different volumes of 40 mM AuCl<sub>3</sub> solutions: (a, b) 0.4, (c, d) 1.0, and (e, f) 2.0 ml.

Figure 5 shows TEM images of the Pt/Au hybrid nanowires after reacting Pt nanowires with different amount of AuCl<sub>3</sub>. The galvanic replacement reaction resulted in the nucleation and deposition of Au atoms along the Pt nanowires to form an Au

nanoparticles/Pt nanowires hybrid structures. When  $\text{AuCl}_3$  was added from 0.4, 1.0 to 2.0 ml, the average size of Au components increased from  $2.7 \pm 0.9$  nm,  $4.4 \pm 0.7$  nm, to  $4.9 \pm 0.5$  nm. The HRTEM images consistently showed the lattice planes for Au and Pt with lattice spacings of 2.4 and 2.3 Å, respectively, which correspond to the {111} lattice planes in both materials (Figure 5d). Since the mismatch of the lattice constants between Pt and Au is less than 5%, Au atoms could nucleate and grow epitaxially on the Pt nanowires along the  $\langle 111 \rangle$  direction via attachment growth. Moreover, as Pearson reported, the Pt/Au phase diagram exhibits a miscibility gap: the solubility of Au in Pt is only about 4% at ambient temperature, rising to 6% at 973 K. Therefore, during the galvanic replacement reaction, reduced Au atoms display a strong tendency to form segregated Au particles on the Pt surfaces. This phenomenon also may be attributed to the low surface free energy of Au compared with that of Pt, thereby favoring the enrichment by Au on the Pt surfaces.

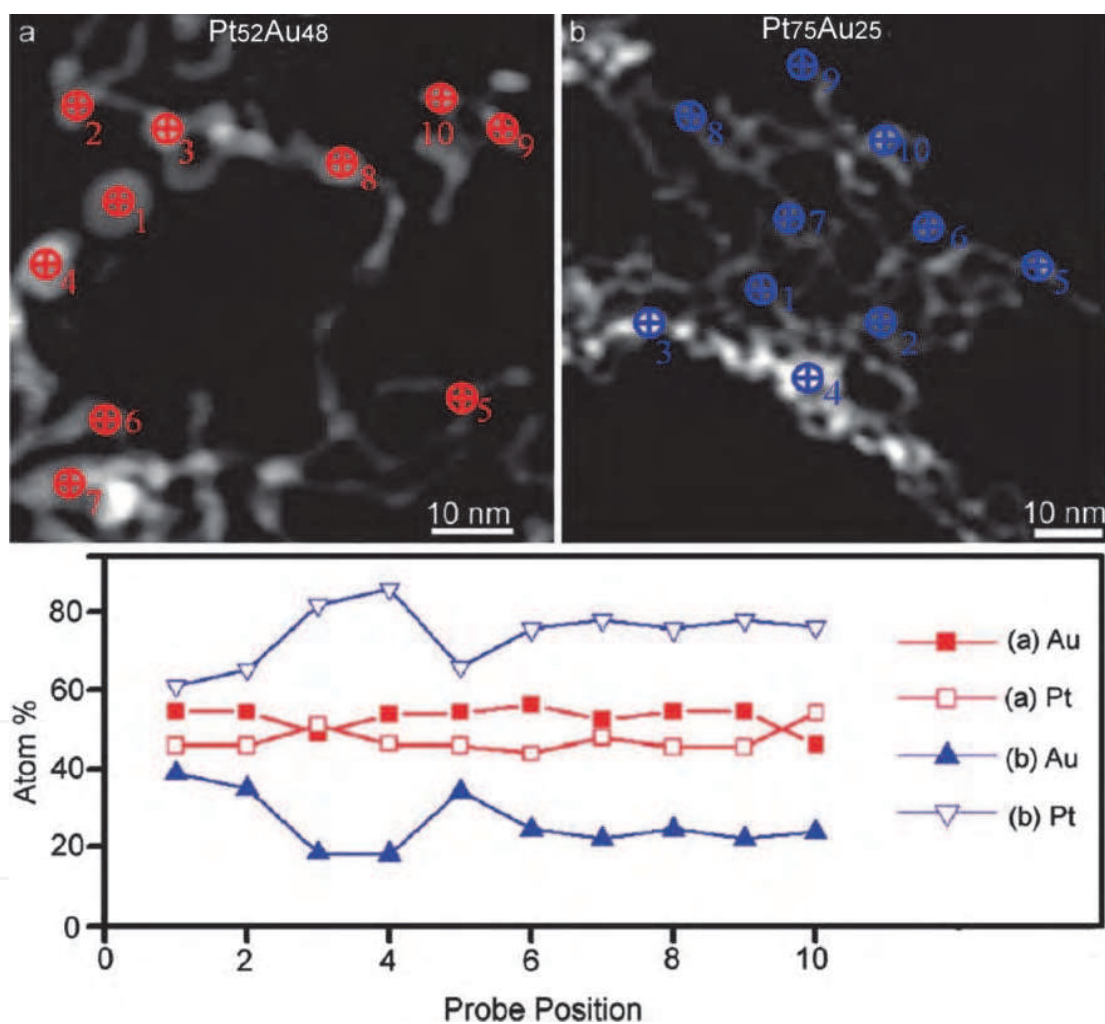


Fig. 6. The dark-field images of (a) Pt<sub>52</sub>Au<sub>48</sub> and (b) Pt<sub>75</sub>Au<sub>25</sub> nanowires, and the elements distributions along individual nanowire assessed by STEM-EDS analysis.

To explore the distributions of the Au and Pt within the Pt/Au alloy nanowires, individual Pt<sub>52</sub>Au<sub>48</sub> and Pt<sub>75</sub>Au<sub>25</sub> nanowires were assessed along the nanowire direction by the probe analysis in the STEM-EDS mode as shown in Figure 6. As illustrated, the contents of Pt and Au were determined at ten sites for either nanowire. Average chemical compositions of

$\text{Pt}_{47\pm 3}\text{Au}_{53\pm 3}$  and  $\text{Pt}_{74\pm 7}\text{Au}_{26\pm 7}$  were identified. The close correspondence of the EDS analysis results obtained from individual nanowires and from their large area assemblies, demonstrates the high degree of homogeneity in chemical composition over a large quantity of as-made  $\text{Pt}_{52}\text{Au}_{48}$  and  $\text{Pt}_{75}\text{Au}_{25}$  nanowires.

The segregation between Pt and Au in Pt/Au hybrid nanowires is evidenced by the scanning transmission electron microscopy–energy dispersive spectroscopy (STEM–EDS) measurements shown in Figure 7.

The STEM–EDS analysis revealed compositional variation along the long axis of the hybrid nanostructures. As illustrated, the contents of Pt and Au were determined for eight sites, located at the tip and along the tail. We found that, except at the site situated in the interface between the tip and tail where both Pt and Au signals were detected (2nd site), there was distinct segregation; Au was detected only at the tip region (1st site), and Pt only was recorded in the tail region, that is, the third to the eighth site.

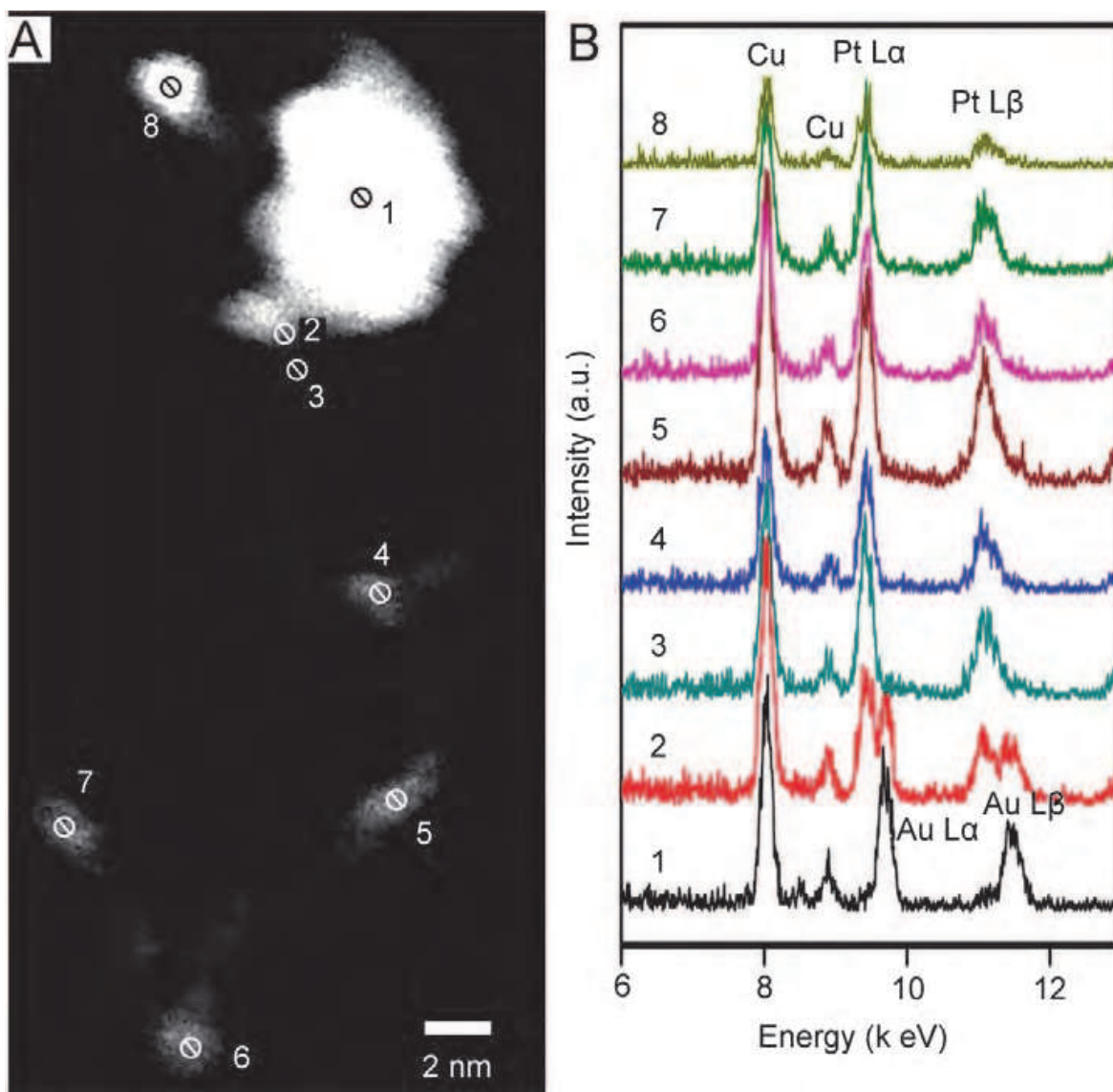


Fig. 7. (A) STEM image of a Pt/Au hybrid nanostructures obtained by titrating the Pt nanowires with 1.0 ml of 40 mM  $\text{AuCl}_3$  solutions and (B) its EDS spectra.

### 3.2 UV–vis spectroscopy analysis

The existence and size changing of Au components in Pt/Au hybrid nanowires were further evidenced from ultraviolet-visible (UV-vis) absorption studies (Figure 8a). As expected, pronounced gold characteristic peaks are obtained for these Pt/Au hybrids. With the increase in concentration of Au, the intensity of the surface plasmon resonance (SPR) peaks which characteristic of gold increased, and the SPR peak positions shifted to higher wavelength. This spectroscopic evidence further confirms the increased size of the Au components in Pt/Au hybrids as the addition of AuCl<sub>3</sub> rose.

We also performed a UV-vis absorption study of pure Pt, Pt<sub>52</sub>Au<sub>48</sub> and Pt<sub>75</sub>Au<sub>25</sub> nanowires as shown in Figure 8b. As expected, pronounced absorption peaks characteristic of gold are obtained for Pt<sub>52</sub>Au<sub>48</sub> and Pt<sub>75</sub>Au<sub>25</sub>. Moreover, the intensity of the surface plasmon resonance (SPR) peak of gold was more pronounced, and shifted to higher wavelength in the gold rich Pt<sub>52</sub>Au<sub>48</sub>. This spectroscopic evidence further confirmed the increased alloying of Au with Pt from Pt<sub>75</sub>Au<sub>25</sub> to Pt<sub>52</sub>Au<sub>48</sub>. Although we intended to synthesize Pt/Au nanowires with higher Au atomic ratios, instead a mixture of nanowires and spherical nanoparticles with various sizes was obtained. The UV-vis absorption performed on this mixture showed a broadened peak between 510 nm and 550 nm, indicating the coexistence of Pt/Au and Au nanomaterials. Because the equilibrium phase diagram is size dependent, our data obtained from PtAu nanowires which are 2~3 nm in length indicate that ~50 atomic% of Au might be the upper limit of the equilibrium concentration of Au in Pt, beyond which phase segregation occurs.

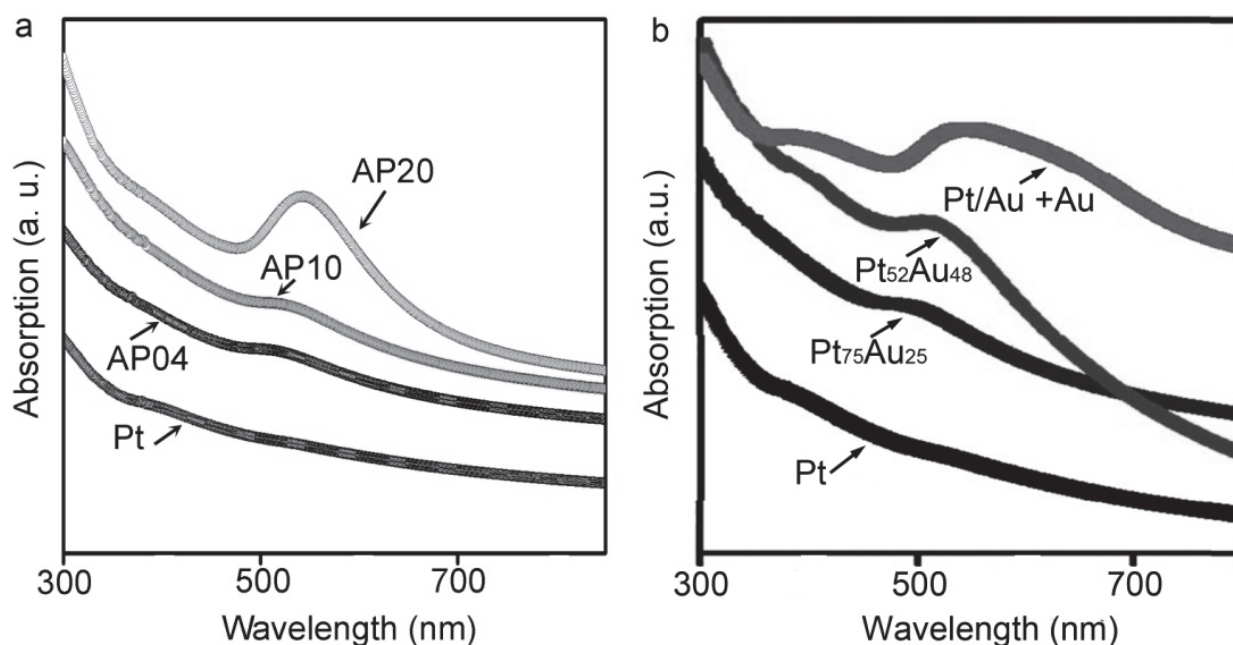


Fig. 8. (a) The UV-vis absorption spectrum of Pt nanowires and Pt/Au hybrid nanostructures obtained by titrating the Pt nanowires with different volumes of 40 mM AuCl<sub>3</sub> solutions: (AP04) 0.4, (AP10) 1.0, and (AP20) 2.0 ml; (b) UV-vis absorption spectrum of as-made Pt, Pt<sub>52</sub>Au<sub>48</sub>, Pt<sub>75</sub>Au<sub>25</sub> nanowires, and mixture of nanowires and Au nanoparticles.

### 3.3 EXAFS characterization

X-ray absorption spectroscopy (XAS) is a well-established technique which provides element specific information on the electronic and structural properties for metallic nanostructures through its two modifications, X-ray absorption near edge structure (XANES) and extended X-ray absorption fine structure (EXAFS).

The EXAFS region, defined as a spectrum region between several hundreds of eV to ~1000 eV above the absorption edge, contains the structural information for coordination environment around the absorbing element. Such parameters including ligand types, coordination numbers, bond distance and disorders can be determined by EXAFS analysis. Simultaneous analysis of EXAFS for both elements in bimetallic nanostructures supply the information of the heterogeneous as well as homogeneous metallic bondings, thus providing evidence to determine the architecture of the bimetallic materials: phase segregation, alloy or core-shell structure (Frenkel, 2007).

Although the morphology and chemical structure of Pt/Au nanowires were verified by TEM and EDS in previous sections, details of the precise crystalline structure such as the Au and Pt distribution and/or coordination inside the nanowires, which is crucial to its physical properties, has not been determined. So we conducted EXAFS studies at both Pt L<sub>3</sub> and Au L<sub>3</sub> edges. The simultaneous, multiple edge (Pt and Au) analysis was employed by fitting theoretical FEFF6 signals of first-nearest-neighbor (1NN) scatterings to the experimental data in r-space while properly accounting for the leakage of Pt L<sub>3</sub> to Au L<sub>3</sub> edge EXAFS. The passive electron reduction factors ( $S_0^2$ ) for both elements are fixed at the values found from fits to their respective foil standards. Several parameters describing electronic properties (e.g. Correction to the photoelectron energy origin) and local structural environment (coordination numbers (N), bond lengths (R) and their mean-squared relative deviation ( $\sigma^2$ ) around absorbing atoms are obtained from the analysis. Such multiple dataset fitting (MDS) analysis is widely applied to all types of bimetallic systems since the additional constraints derived from the association between the two component elements (e.g. Bond lengths and bond length disorders for the heterogeneous bonds are constrained to be the same as measured from either edge) significantly lower the number of fitting variables, improving the confidence levels of fitting analysis effectively.

Pt/Au bimetallic system in EXAFS analysis represents a unique case which features overlapping absorption edges. In specific, Pt L<sub>3</sub> edge (11,564 eV) and Au L<sub>3</sub> edge (11,919 eV) are so close (energy gap only 355 eV) that the Pt L<sub>3</sub> EXAFS leaks to Au L<sub>3</sub> EXAFS data. The MDS analysis of such case is performed by a simultaneous fit of both Pt L<sub>3</sub> and Au L<sub>3</sub> edges, which account three contributions: (1) the Pt EXAFS in the Au L<sub>3</sub> edge before the Au L<sub>3</sub> edge; (2) the Au EXAFS in the Au L<sub>3</sub> edge; and (3) the Pt EXAFS in the Au L<sub>3</sub> edge. Since (1) and (2) describe the same coordination environments they are strictly constrained mathematically; and a scaling factor  $F = \Delta\mu_{0,Pt} / \Delta\mu_{0,Au}$  is used as the Pt EXAFS contribution in Au EXAFS is calculated, to compensate the different magnitude of edge steps for Pt and Au L<sub>3</sub> EXAFS data. As well, a correction value (eV) at  $\Delta E_{0,Pt} - (358 + \Delta E_{0,Au})$  to threshold energy of Au L<sub>3</sub> is added for Pt L<sub>3</sub> EXAFS in Au L<sub>3</sub> edge data to correct energy grid of this contribution, where 358 eV is the difference between empirical threshold energies for Pt L<sub>3</sub> and Au L<sub>3</sub> edge, which were set at 11562 eV and 11920 eV respectively in the this analysis. Additionally, for metallic bonds, only effective structural

parameters for each element were varied: the coordination numbers ( $N_{Pt-M}$ ,  $N_{Au-M}$ ), bond lengths ( $R_{Pt-M}$ ,  $R_{Au-M}$ ) and their disorders ( $\sigma_{Pt-M}^2$ ,  $\sigma_{Au-M}^2$ ), due to the similarity of backscattering amplitudes of Pt-Pt and Pt-Au as well as Au-Au and Au-Pt pairs. Detail of this analysis approach can be found in reference.<sup>24</sup> Figure 9 depicts two examples of Pt/Au EXAFS data and their corresponding fits in r-space, along with individual contribution from each scattering path (Pt-M, Au-M, and Pt-O and Au-O) in both Pt and Au L<sub>3</sub> edge data.

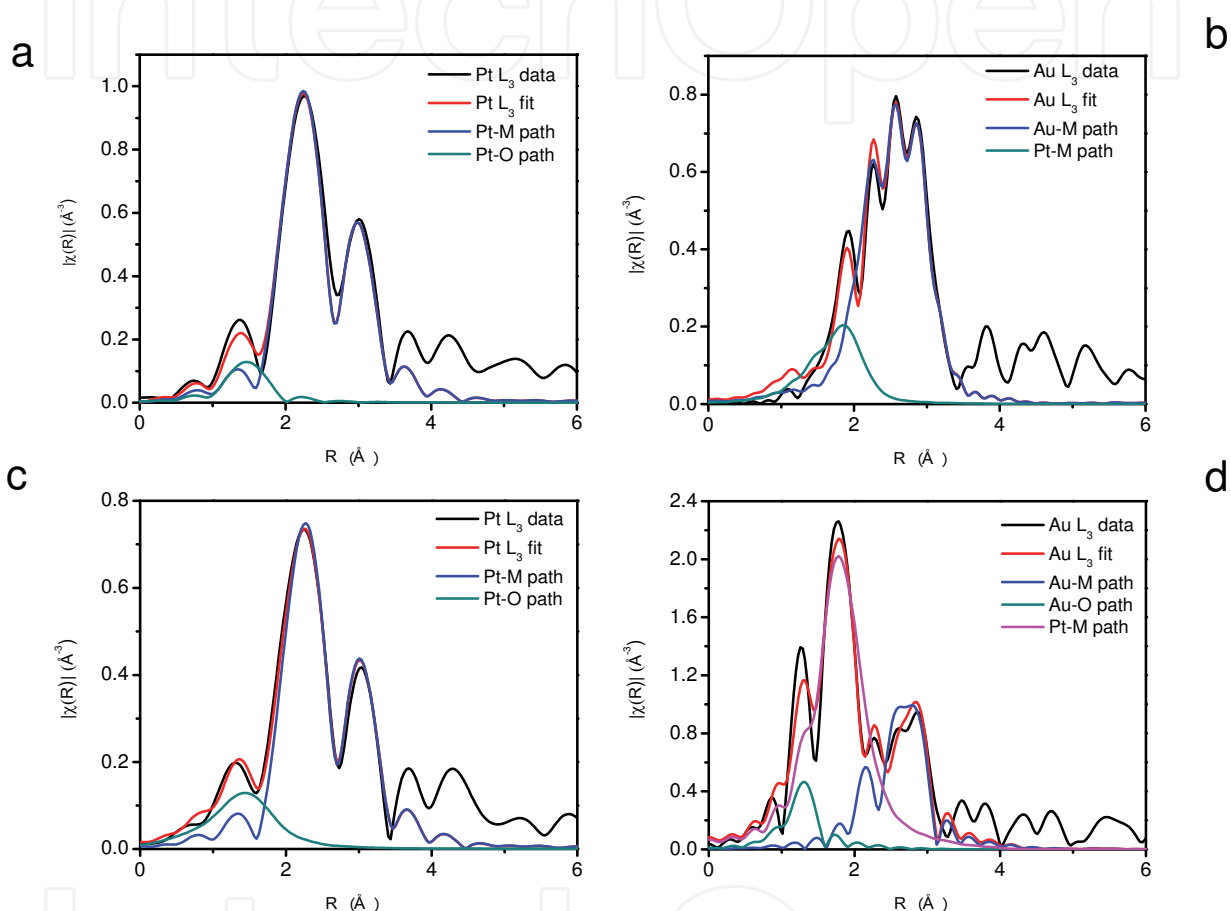


Fig. 9. Selected set of EXAFS data in R space and fits for Au/Pt bimetallic nanoparticles (a, b) AP10 and (c, d) AP04. (a, c) Pt data and fit; (b, d) Au data and fit. The comparison of Au edge EXAFS shows that Pt L<sub>3</sub> leakage contributes much extensively in AP04 than in AP10. Also shown is that the fitting of Au data for AP04 was complicated by nonmetallic bonding to Au in addition to Pt leakage.

The best fit values of structural parameters (coordination numbers, first nearest neighbor distances and their mean squared disorders,  $\sigma^2$ ) for Pt/Au alloy nanowires and Pt/Au hybrid nanowires are listed in the Table 1 and Table 2, respectively. For Pt<sub>52</sub>Au<sub>48</sub> nanowires, the first-nearest-neighbor (1NN) Pt-metal coordination number ( $N_{Pt-M} \equiv N_{Pt-Au} + N_{Pt-Pt}$ ) is  $9.1 \pm 0.6$ , comparable to that of Au-metal coordination number ( $N_{Au-M} \equiv N_{Au-Au} + N_{Au-Pt} = 9.7 \pm 1.9$ ). The fact that  $N_{Pt-M} \approx N_{Au-M}$ , within the error bars, implies the formation of a homogeneous Pt/Au alloy. Thus, Au or Pt do not segregate to different macroscopic regions within the nanostructure (e.g., to the center or surface). Our measurements of Pt<sub>75</sub>Au<sub>25</sub>

nanowires suggest a heterogeneous distribution of Au and Pt atoms inside the nanowires. The observed relationship:  $N_{\text{Pt-M}} (5.3 \pm 0.6) < N_{\text{Au-M}} (9.4 \pm 1.9)$  indicates that Au atoms tend to segregate toward the core of the  $\text{Pt}_{75}\text{Au}_{25}$  nanowires, leading to a heterogeneous nanostructure with a Au-rich and highly coordinated core and a less coordinated Pt-rich shell, since the atoms on the surface have fewer neighbors (or lower coordination number) than those in the core.

samples	Pt foil	$\text{Pt}_{75}\text{Au}_{25}$	$\text{Pt}_{52}\text{Au}_{48}$	Au foil
$N_{\text{Pt-M}}$	12 <sup>a</sup>	5.3 (6)	9.1 (6)	
$N_{\text{Au-M}}$		9.4 (1.9)	9.7 (1.9)	12 <sup>a</sup>
$N_{\text{Pt-O}}$		0.8 (7)		
$N_{\text{Au-O}}$		0.9 (5)		
$R_{\text{Pt-M}} (\text{Å})$	2.775 (2)	2.750 (6)	2.767(5)	
$R_{\text{Au-M}} (\text{Å})$		2.84 (1)	2.82(1)	2.877(3)
$R_{\text{Pt-O}} (\text{Å})$		1.95 (4)		
$R_{\text{Au-O}} (\text{Å})$		1.77 (2)		
$\sigma^2_{\text{Pt-M}} (\text{Å}^2)$	0.0050(1)	0.0024(4)	0.0105(8)	
$\sigma^2_{\text{Au-M}} (\text{Å}^2)$		0.0075(11)	0.0086(18)	0.0081(2)
$\sigma^2_{\text{Pt-O}} (\text{Å}^2)$		0.0077(140)		
$\sigma^2_{\text{Au-O}} (\text{Å}^2)$		0.0029(52)		

<sup>a</sup> 1NN coordination number was fixed at 12 for Pt and Au bulk standard analyses.

Table 1. Best Fit Results Obtained by EXAFS Analysis for Pt/Au Bimetallic Nanowires

The results from EXAFS analysis for Pt/Au hybrid bimetallic nanostructures are consistent with the elemental segregation revealed by electron microscopy. The Pt-Pt and Pt-O coordination numbers for the starting material (i.e. Pt nanowires) are  $7.2 \pm 0.4$  and  $0.28 \pm 0.2$ , respectively, which agrees with Pt nanowires of 2.3 nm in width and a small amount of oxide on the structure surface. Coordination of  $7.4 \pm 0.4$  and  $8.0 \pm 0.3$  were resulted for Pt-M in AP04 and AP10, indicating that the width of Pt nanowires did not change significantly from the starting phase when 0.4 ml and 1.0 ml  $\text{AuCl}_3$  was added. On the contrary, dramatic increase of Au-M coordination number from  $5.9 \pm 2.5$  in AP04 to  $9.8 \pm 2.1$  in AP10 was observed, which well corroborates the Au nanoparticle growth from  $2.7 \pm 0.9$  to  $4.4 \pm 0.7$  nm found from electron microscopy study. No significant change in Au-M coordination number ( $8.7 \pm 0.7$ ) was observed for AP20 compared to that of AP10, consistent with the microscopic evidence where Au particle sizes were determined to only change from  $4.4 \pm 0.7$  nm to  $4.9 \pm 0.5$  nm as  $\text{AuCl}_3$  concentration was doubled from 10 ml to 20 ml. A noticeable increase in Pt-M coordination number ( $10.5 \pm 1.1$ ) observed in AP20 relative to that in AP04 and AP10 may imply the increased Pt-Pt and Pt-Au interactions due to shortened nanowires and more Au decorations on the surface of Pt nanowire. As expected, Pt-M bonds in all hybrid samples show the contraction from bulk Pt-Pt bond, in a similar degree; while the Au-M bond in AP04 shrinks the most with the smallest size of particles. No dramatic increase in bond length disorders are shown in those Au/Pt hybrid samples compared to bulk structures, which may be explained by the non-traditional nanostructure of Pt nanowires and more complete segregation between Pt and Au in these hybrid structures.

Samples	Pt nanowires	PtAu (0.4ml)	PtAu (1.0ml)	PtAu (2.0ml)
$N_{\text{Pt-M}}$	7.2 (4)	7.4 (4)	8.0 (3)	10.5 (1.1)
$N_{\text{Pt-O}}$	0.28 (2)	1.2 (1.0)	1.1 (6)	0.3 (0.3)
$N_{\text{Au-M}}$		5.9 (2.5)	9.4 (1.9)	8.7 (7)
$N_{\text{Au-O}}$		0.6 (0.7)		
$R_{\text{Pt-M}}(\text{Å})$	2.743 (3)	2.749 (5)	2.758 (5)	2.744 (7)
$R_{\text{Pt-O}}(\text{Å})$	1.963 (28)	1.950 (35)	1.937 (22)	1.916 (51)
$R_{\text{Au-M}}(\text{Å})$		2.831 (13)	2.833 (13)	2.844 (5)
$R_{\text{Au-O}}(\text{Å})$		1.686 (36)		
$\sigma^2_{\text{Pt-M}}(\text{Å}^2)$	0.0073 (3)	0.0053 (3)	0.0059 (2)	0.0061 (6)
$\sigma^2_{\text{Pt-O}}(\text{Å}^2)$	0.0040 (63)	0.0260 (182)	0.0245 (166)	0.0000 (74)
$\sigma^2_{\text{Au-M}}(\text{Å}^2)$		0.0043 (19)	0.0090 (13)	0.0085 (5)
$\sigma^2_{\text{Au-O}}(\text{Å}^2)$		0.0000 (70)		

Table 2. Best Fit Results Obtained By EXAFS Analysis for Pt-Au hybrid Nanowires

#### 4. Electronic structure characterized by X-ray Absorption Near Edge Spectroscopy (XANES)

XANES is a powerful X-ray absorption spectroscopy technique for investigating charge transfer between distinctive elements as well as oxidation states of specific element within the nanomaterials. In contrast to EXAFS, the XANES energy range is only approximately 5~150 eV above the edge, much lower than that of EXAFS region. By analyzing these absorption signals in XANES, one can extract abundant chemical information of the studied material, like formal valence, coordination environment, the unoccupied band structure of a material, and fingerprint a mixture of sites/compounds (e.g. oxidation state determination), etc.

Since XANES is sensitive to the local electronic structure, it has been used to study the electronic redistribution or charge transfer upon alloying between various compounds. Obviously, it would also be the desirable technique to study the electronic structure of those Pt/Au hybrid nanowires. Despite the fact that Au metal with filled  $d^{10}$  orbital usually doesn't exhibit an intense white line (the first feature in the absorption edge) at  $L_3$  edge thresholds compared with unfilled  $d^9$  metals (e.g. Pt), the orbital  $s$ - $p$ - $d$  hybridization results in a  $5d^{10-x}6(sp)^{1+x}$  electron configuration, leading to a potentially noticeable increase of white line intensity. The changes of the number of holes in the  $d$  band reflect charge transfer between various Pt/Au hybrid nanostructures. Therefore, enhancement of the white line intensity from both Pt and Au  $L_3$  edges can thus be used as a sensor, to detect and quantify the hybrid formation. Figure 10 shows normalized Pt  $L_3$  edge XANES spectra of Pt/Au hybrids and those of Au and Pt foils for reference. It can be seen that the strength of the Au white line feature in  $L_3$  edge is noticeably lower than that of pure Au

foil as the amount of Au components decreased. Since white line features in Au  $L_3$  edge arise from  $2p_{3/2}$  to  $5d_{5/2}$  dipole transitions, the observations indicate a decrease in the number of unoccupied states of d character at the Au site upon the dilution of Au components in Pt nanowires. An opposite trend is seen at the Pt  $L_3$  edge, where the white line feature is higher than that of the pure Pt foil upon the dilution of Au concentration in Pt/Au hybrids. The data can be further interpreted in terms of the holes population above the Fermi level i.e., the d-charge depletion at the Pt site is accompanied by the d-charge gain at the Au site. The d charge gain at the Au site should be comparable to the charge loss at the Pt sites on the basis of electronic charge neutrality consideration.

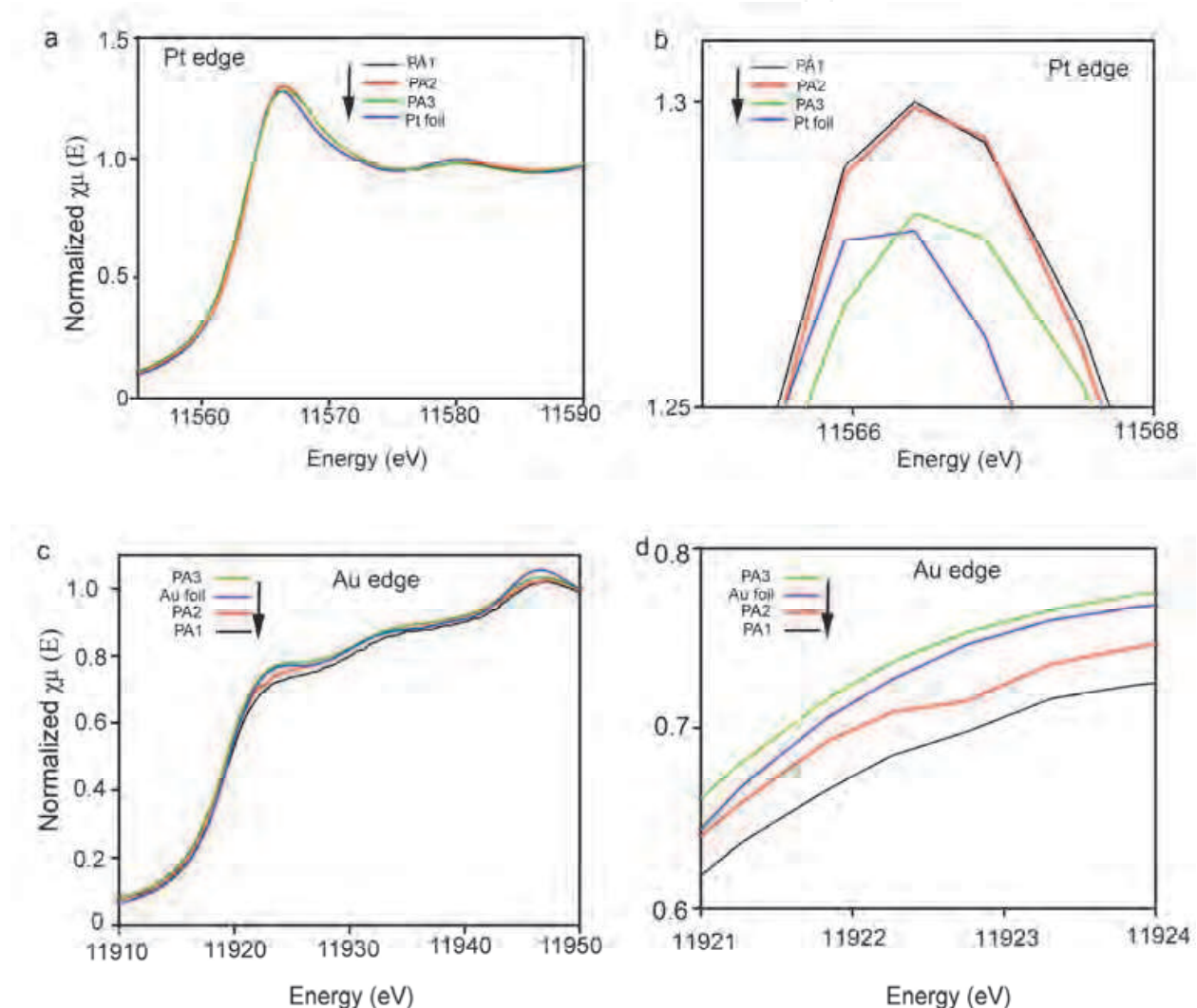


Fig. 10. Normalized XANES spectra of (a, b) Pt and (c, d) Au in the Pt/Au hybrid nanowires obtained by titrating the Pt nanowires with different volumes of 40 mM  $\text{AuCl}_3$  solutions: (AP04, black) 0.4, (AP10, red) 1.0, and (AP20, green) 2.0 ml, as well as in the Au (blue) and Pt (blue) foils.

It is important to mention that the white line intensity is known to increase as the particle size decreases. That is, the partial positive charge resulting from charge transfer is

distributed over fewer atoms (smaller particles), resulting in a greater increase in the d-hole population above the Fermi level relative to that of the larger particles. However, our data have clearly different origin as the size-effect which would cause the both Au and Pt white lines increase relative to the bulk as sizes decrease, contrary to what we observed. Moreover, the charge transfer between Pt/Au in hybrid structure seems totally different from that happened in Au bimetallic alloys such as Ag/Au, Al/Au or Ga/Au, where Au sites always lose d charges locally and therefore exhibit a more intense white line than Au foil. This unusual and interesting electronic behavior in Pt/Au hybrids is rather unexpected and deserves further investigations.

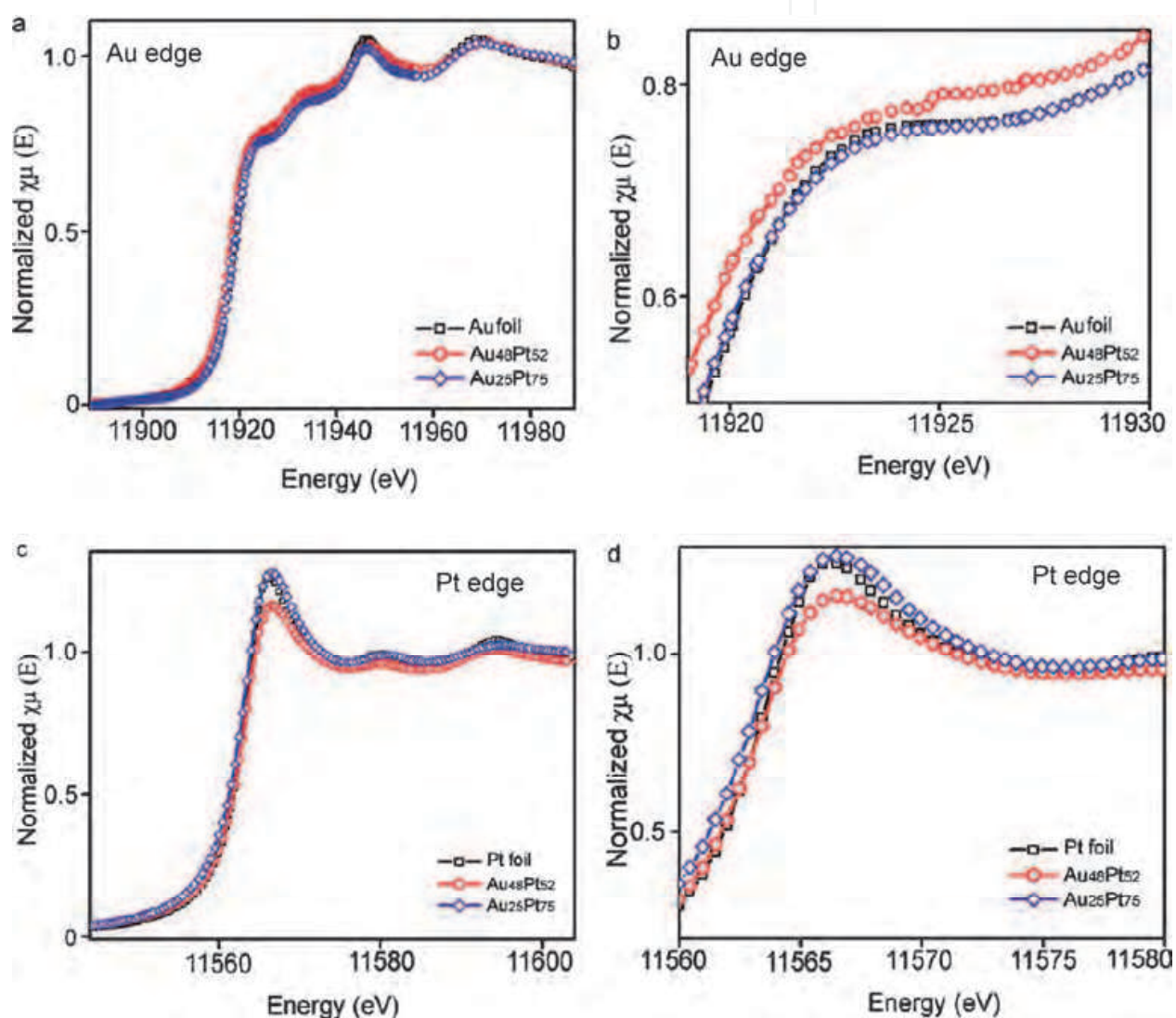


Fig. 11. XANES spectrum of (a, b) Au L<sub>3</sub> edge and (c, d) Pt L<sub>3</sub> edge of as-made Pt<sub>52</sub>Au<sub>48</sub> (nanowires), Pt<sub>75</sub>Au<sub>25</sub> (nanowires), Pt (foil reference), and Au (foil reference).

The XANES study of Pt/Au alloy nanowires (specifically, Pt<sub>52</sub>Au<sub>48</sub>), however, revealed a rather unexpected opposite trend of charge transfer directions compared with Pt/Au hybrids as shown in Figure 11. For Pt<sub>52</sub>Au<sub>48</sub> nanowires, the strength of the Au white line feature is noticeably higher than that of pure Au foil. Since features in the white line at the

Au  $L_3$  edge arise from  $2p_{3/2}$  to  $5d_{5/2}$  dipole transitions, our observations indicate a increase in the number of unoccupied states of d character at the Au site upon the  $Pt_{52}Au_{48}$  alloy formation. An opposite trend is seen at the Pt  $L_3$  edge, where the white line feature is lower than that of the pure Pt foil. The Pt and Au  $L_3$  edges shifted in opposite directions are the consequence of Pt/Au alloy formation. The data can be further interpreted in terms of the hole population above the Fermi level, in which sense the d-charge depletion at the Au site is accompanied by the d-charge gain at the Pt site. Electronic charge neutrality requires that the d charge gain at the Pt site should be comparable to the charge loss at the Au sites. In contrast, the Au and Pt white line features found in  $Pt_{75}Au_{25}$  nanowires are very close to those found in Au and Pt foil. The bulk-like XANES curves around the absorption edge indicate no apparent charge transfer between Au and Pt atoms, as well as between Pt/Au and octadecylamine in  $Pt_{75}Au_{25}$  nanowires. The electronic structure of PtAu alloy nanoparticles supported on the metal oxides has been studied by Van Bokhoven and coworkers, finding a charge transfer between Au and Pt similar to our results on Pt/Au free-standing nanowires (Bus & van Bokhoven, 2007). However, the charge transfer of Pt/Au hybrid phase-segregated nanostructures is totally different from that of an alloyed structure. As we discussed in earlier sections, d-charge depletion at the Pt site and d-charge gain at the Au site was found in Pt/Au hybrid with complete Au and Pt phase-segregation. We believe that the distinct electronic structures found in the two materials can be attributed to their different crystalline structures. Since Au has a higher electronegativity than Pt, in Pt/Au hybrid phase-segregated nanowires, Pt loses electrons to Au. In Pt/Au alloyed nanowires, alloying between Au and Pt drives the system towards the "covalent limit", where the d bandwidth is much larger than the energy separation of the d bands, forcing Pt and Au towards equal electron counts in the alloy (Bus & van Bokhoven, 2007). These findings dramatically highlight the intriguing structure-property relationship of nanoscaled electronic materials.

## 5. Conclusion

In summary, we synthesized Pt ultrathin nanowires, and Au/Pt alloyed and hybrid nanowires heterogeneous structures via a phase transfer wet chemistry synthetic method. Using a combination of techniques, including STEM equipped with EDS, UV-vis spectroscopy, and synchrotron-based XANES and EXAFS, we identified the stoichiometry-dependent heterogeneous crystalline structures, as well as electronic structures with respect to the charge transfer between Pt and Au within both nanowires. In particular, we observed d-charge depletion at the Au site and the d-charge gain at the Pt site in  $Au_{48}Pt_{52}$  alloyed nanowires. On the other hand, an opposite charge transfer trend was found in Au/Pt hybrid nanowires, where we observed d-charge depletion at the Pt site and the d-charge gain at the Au site. We have presented here a comprehensive study of the relationships among heterogeneous crystalline structure and electronic structure. Our studies are highly encouraging that new families of bimetallic nanosystems may be developed to sustain the needs of emerging technologies such as electronics and catalysis, where there is a continuous drive to find nanomaterials with ever more exotic electronic and catalytic properties, and where the assembly of these fundamental building blocks can lead to new types of functionality.

## 6. Acknowledgments

This work is supported by the University of New Hampshire. Dr. Wang acknowledges support by the U.S. Department of Energy grant No. DE-FG02-03ER15476. Use of the National Synchrotron Light Source, Brookhaven National Laboratory, was supported by the U.S. Department of Energy, Office of Science, Office of Basic Energy Sciences, under Contract DE-AC02-98CH10886 and beam lines X19A/X18B are partly supported by Synchrotron Catalysis Consortium under contract DE-FG02-05ER15688.

## 7. References

- Ahmadi, T. S.; Wang, Z. L.; Green, T. C.; Henglein, A.; ElSayed, M. A., (1996). Shape-controlled synthesis of colloidal platinum nanoparticles. *Science*, Vol. 272, pp 1924-1926.
- Casado-Rivera, E.; Volpe, D. J.; Alden, L.; Lind, C.; Downie, C.; Vazquez-Alvarez, T.; Angelo, A. C. D.; DiSalvo, F. J.; Abruna, H. D., (2004). Electrocatalytic activity of ordered intermetallic phases for fuel cell applications. *Journal of the American Chemical Society*, Vol. 126, pp 4043-4049.
- Cozzoli, P. D.; Manna, L., (2005). Asymmetric nanoparticles - Tips on growing nanocrystals. *Nature Materials*, Vol. 4, pp 801-802.
- Xia, Y. N.; Yang, P. D.; Sun, Y. G.; Wu, Y. Y.; Mayers, B.; Gates, B.; Yin, Y. D.; Kim, F.; Yan, Y. Q., (2003). One-dimensional nanostructures: Synthesis, characterization, and applications. *Advanced Materials*, Vol. 15, pp 353-389.
- Zhong, C. J.; Maye, M. M., (2001). Core-shell assembled nanoparticles as catalysts. *Advanced Materials*, Vol. 13, pp 1507-1511.
- Nashner, M. S.; Frenkel, A. I.; Adler, D. L.; Shapley, J. R.; Nuzzo, R. G., (1997). Structural characterization of carbon-supported platinum-ruthenium nanoparticles from the molecular cluster precursor  $\text{PtRu}_5\text{C}(\text{CO})_{16}$ . *Journal of the American Chemical Society*, Vol. 119, pp 7760-7771.
- Shibata, T.; Bunker, B. A.; Zhang, Z. Y.; Meisel, D.; Vardeman, C. F.; Gezelter, J. D., (2002). Size-dependent spontaneous alloying of Au-Ag nanoparticles. *Journal of the American Chemical Society*, Vol. 124, pp 11989-11996.
- Greeley, J.; Mavrikakis, M., (2006). Near-surface alloys for hydrogen fuel cell applications. *Catalysis Today* Vol. 111, pp 52-58.
- Knudsen, J.; Nilekar, A. U.; Vang, R. T.; Schnadt, J.; Kunkes, E. L.; Dumesic, J. A.; Mavrikakis, M.; Besenbacher, F., (2007). A Cu/Pt near-surface alloy for water-gas shift catalysis. *Journal of the American Chemical Society*, Vol. 129, pp 6485-6490.
- Brust, M.; Walker, M.; Bethell, D.; Schiffrin, D. J.; Whyman, R., (1994). Synthesis of Thiol-Derivatized Gold Nanoparticles in a 2-Phase Liquid-Liquid System. *Journal of the Chemical Society, Chemical Communications*, pp 801-802.
- Frenkel, A., (2007). Solving the 3D structure of metal nanoparticles. *Zeitschrift Fur Kristallographie*, Vol. 222, pp 605-611.

Bus, E.; van Bokhoven, J. A., (2007). Electronic and geometric structures of supported platinum, gold, and platinum - Gold catalysts. *Journal of Physical Chemistry C*, Vol. 111, pp 9761-9768

IntechOpen

IntechOpen



## **Nanowires - Fundamental Research**

Edited by Dr. Abbass Hashim

ISBN 978-953-307-327-9

Hard cover, 552 pages

**Publisher** InTech

**Published online** 19, July, 2011

**Published in print edition** July, 2011

Understanding and building up the foundation of nanowire concept is a high requirement and a bridge to new technologies. Any attempt in such direction is considered as one step forward in the challenge of advanced nanotechnology. In the last few years, InTech scientific publisher has been taking the initiative of helping worldwide scientists to share and improve the methods and the nanowire technology. This book is one of InTech's attempts to contribute to the promotion of this technology.

### **How to reference**

In order to correctly reference this scholarly work, feel free to copy and paste the following:

Xiaowei Teng, Wenxin Du and Qi Wang (2011). Synthesis of Pt-Containing Metals Alloy and Hybrid Nanowires and Investigation of Electronic Structure Using Synchrotron-Based X-Ray Absorption Techniques, Nanowires - Fundamental Research, Dr. Abbass Hashim (Ed.), ISBN: 978-953-307-327-9, InTech, Available from: <http://www.intechopen.com/books/nanowires-fundamental-research/synthesis-of-pt-containing-metals-alloy-and-hybrid-nanowires-and-investigation-of-electronic-structu>

**INTECH**  
open science | open minds

### **InTech Europe**

University Campus STeP Ri  
Slavka Krautzeka 83/A  
51000 Rijeka, Croatia  
Phone: +385 (51) 770 447  
Fax: +385 (51) 686 166  
[www.intechopen.com](http://www.intechopen.com)

### **InTech China**

Unit 405, Office Block, Hotel Equatorial Shanghai  
No.65, Yan An Road (West), Shanghai, 200040, China  
中国上海市延安西路65号上海国际贵都大饭店办公楼405单元  
Phone: +86-21-62489820  
Fax: +86-21-62489821

© 2011 The Author(s). Licensee IntechOpen. This chapter is distributed under the terms of the [Creative Commons Attribution-NonCommercial-ShareAlike-3.0 License](#), which permits use, distribution and reproduction for non-commercial purposes, provided the original is properly cited and derivative works building on this content are distributed under the same license.

IntechOpen

IntechOpen